

Direct Observation of the Local-Field-Enhanced Surface Photochemical Reactions

C. J. Chen and R. M. Osgood

*Columbia Radiation Laboratory and Department of Electrical Engineering, Columbia University,
New York, New York 10027*

(Received 19 November 1982)

The enhancement of photochemical reactions on surface-supported metallic particles is reported. The result is obtained by uv photodissociation of organometallic molecules adsorbed on the supporting surface. Transmission electron-microscope micrographs of the resulting photodeposited film reveal enhanced deposition on and near the metal particles, and a clear interference pattern resulting from the mixing of the incident and reradiated light. The importance of the particle plasma resonance is described.

PACS numbers: 82.50.-m

In this Letter, we report a direct observation of a surface-enhanced photochemical reaction. The experiment is motivated in part by the recent studies of enhanced Raman scattering (SERS) on rough metal surfaces.¹ Although the exact mechanism of SERS is still a matter of some controversy, it is clear that much of the enhancement results from a plasma resonance in the metal protrusions on the surface, which in turn greatly magnifies the local optical electric field.² This explanation suggests that a similar enhancement should exist for photochemical phenomena occurring on similarly shaped metal surfaces.

The possibility of such surface-enhanced photochemistry has been discussed theoretically by Nitzan and Brus.³ However, they emphasized that the rapid relaxation occurring on metal surfaces can be expected to quench long-lived photochemically active states. In this Letter, we use the photodecomposition of a metal-alkyl adlayer and its resultant metal deposit to show that enhanced *direct* photochemical reactions can occur in the vicinity of metal spheroids.

According to the above discussion two conditions have to be fulfilled to observe such an enhanced reaction. First, the reaction chosen must involve a short-lived dissociative state; that is, the chemical reaction should occur in 10^{-14} – 10^{-13} s. Second, the frequency of the incident light should be at a plasma resonance of the metal structure. The resonant frequency of a metal ellipsoid depends sharply on the dielectric constants of the metal and the shape of the metal feature.

While silver has been almost exclusively used in SERS studies, the resonance frequencies typical of silver structures are too low to affect most direct one-photon photochemical reactions. However, optical and electron-beam energy-loss spectra⁴ show that several other metals such as

Cd, In, and Al do exhibit sharp absorption peaks, as a result of a plasma resonance, in the mid-uv region⁴; see Table I. For small particles the resonant frequency, ω_r , depends on the particle shape; see below. The resonant frequency ω_r for a sphere of a metal which can be described by a Drude-type free-electron model is $\omega_r = \omega_p / \sqrt{3}$. Table I also lists $\omega_p / \sqrt{3}$ for the same metals, as well as the experimental value of ω_r .

The photochemical reaction chosen was the photodissociation of Me₂Cd (dimethyl cadmium) by a 257-nm laser beam. The photodissociation mechanism of Me₂Cd has been studied carefully and the required instantaneous dissociation mechanism was confirmed.⁶ The absorption spectra of the Me₂Cd vapor and physisorbed layer have also been recently studied.⁷ While both phases exhibit adsorption at 257 nm, the adlayer adsorption is stronger by a factor of 5.

The experiment consisted of observing the distribution of photodeposited cadmium in the vicinity of metallic spheres supported on a thin dielectric substrate. The spheres were made of two metals, cadmium and gold, which possess, respectively, a very strong plasma resonance and no plasma resonance near 257 nm.

TABLE I. Plasma resonance energies (eV) of several metals, calculated from the data given in Refs. 4 and 5. E_p is defined as the photon energy at which $\epsilon_1 = 0$; E_r for a sphere is the energy at which $\epsilon_1 = -2$.

Metal	E_p bulk metal	E_p for sphere	$E_p / \sqrt{3}$
Cd	8.5	5.0	4.9
In	11.4	7.4	6.6
Al	15.0	8.3	8.7
Ag	3.7	3.5	2.1

The cadmium spheres were made on very thin (~ 10 -nm) carbon films, after a procedure by Kimoto *et al.*,⁸ by evaporating 0.5 mg of cadmium metal in a vacuum evaporator filled with 3–5 Torr of pure argon. The film was then separated from the substrate and supported on standard 3-mm-diam copper grids.

The transmission electron micrographs of those cadmium particles showed that the sizes were distributed from 10 to 300 nm. The cadmium particles with diameters less than 100 nm were essentially spherical [Fig. 1(a)]. Those bigger than 100 nm were hexagonal single crystals as previously reported.⁸

The grids with cadmium particles were enclosed in an optical cell with fused-silica windows and filled with 1 Torr of Me_2Cd and 1000 Torr of argon. The cell-fill procedure and pressure were described in Ref. 9. Under these conditions, the dominant contribution of atoms to the photodeposited metal comes from molecules in the surface adlayer. One of the 0.1×0.1 -mm² windows of the grid was then irradiated by a weakly focused 257-nm uv beam from a frequency-doubled argon-ion laser. The grid pattern was aligned with the polarization of the light for identification. The intensity of the uv beam was estimated to be < 1 W/cm²; thus substrate heating was not important. After a 1-min exposure, a thin metal deposition was observed with an optical microscope. The microstructure of the deposited film was then examined again with a transmission electron microscope (TEM) with 1-nm resolution. Figures 1(b), 1(c), and 1(d) show TEM micrographs of the carbon film with the evaporatively deposited Cd particles after a short period of photodeposition from the

$(\text{CH}_3)_2\text{Cd}$ adlayer. The small spherical particles of initial diameters 10–100 nm grew into ellipsoids with their long axes aligned to within $\pm 10^\circ$ along the electric-field vector. During the same period no enhanced growth of either the very small ($a < 5$ nm) or very large ($a > 200$ nm) particles occurred. After much longer periods of exposure the slow growth of the smaller particles into larger ellipsoidal shapes was observed.

Measurements of a large number (> 200) of particles showed that the ellipsoidal growth slowed when the particles grew into a ratio of a/b of 1.80 ± 0.31 and a major axis $2a$ of 110 ± 40 nm. The thin cadmium deposition on the carbon film around these particles showed a regular pattern; there was a zone of weak deposition around each ellipsoid, especially along the particle's equator [Figs. 1(b) and 1(c)].

In experiments using supported gold particles, the initial metal spheroids were of comparable size and shape as for the case of the cadmium structures. However, despite the fact that we were also able to produce photodeposited film under the same circumstances as for the cadmium particles, no ellipsoidal growth occurred from the gold particles.

The growth of the ellipsoidal particles shown in Fig. 1 may be explained after first determining the optical electrical field occurring in the vicinity of metal particles in plasma resonance with the applied field. The electric field near the surface of a metal ellipsoid [Fig. 2(a)] can be calculated by using the electrostatic approximation and by taking into account the (optical) frequency-dependent dielectric constant. For cadmium, optical measurements show that the free-electron-gas model is a reasonable description.⁵ In this case the dielectric function can be represented in the mid-uv region by the Drude formula with reasonable accuracy⁴:

$$\epsilon(\omega) = \epsilon_1(\omega) + i\epsilon_2(\omega) = 1 - \omega_p / \omega(\omega + i/\tau), \quad (1)$$

where ω_p is the plasma resonance frequency of the bulk metal and τ is the relaxation time of the electrons. With use of this frequency-dependent dielectric constant, it can be shown that an ellipsoid, illuminated with the geometry shown in Fig. 1, has resonance frequency

$$\omega_r = \omega_p [(\alpha - \tanh)/\tanh \sinh^2 \alpha]^{1/2}, \quad (2)$$

where $\cosh \alpha = a/b$ and b is the semiminor axis, also smaller than the wavelength of light. The dependence of ω_r on a/b for cadmium is shown

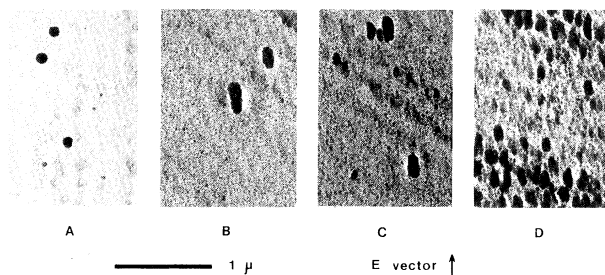


FIG. 1. The TEM photographs of the carbon film with miniature cadmium particles (a) before photochemical deposition, showing randomly distributed spheres; (b), (c), (d) after photochemical deposition, showing elliptical similar growth to similar sizes, well aligned with the electric field of the light.

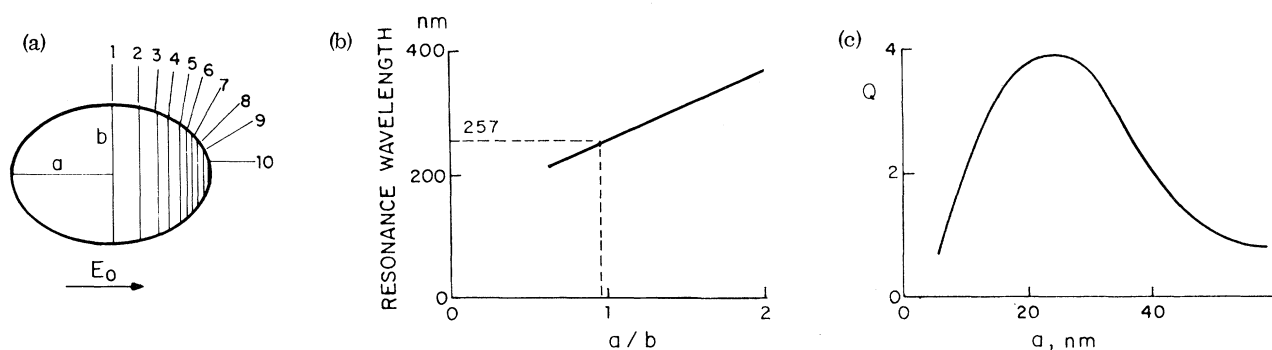


FIG. 2. (a) Distribution of electrical energy density on the surface of a metal particle in an external optical electric field. The numbers show the relative strengths of E^2 , which are proportional to the photodissociation rates at these equipotential lines. (b) Variation of the resonance wavelength of prolate cadmium spheroids with the ratio b/a (using the data of Ref. 5). (c) Variation of the quality factor Q of cadmium spheroids with the size a , $b/a = 1.2$.

in Fig. 2(b).

The quality factor Q of the plasma resonance for the particles is limited not only by the relaxation time τ of the bulk metal, but also by two size-dependent factors. For very small particles, when the size, $l = (ab^2)^{1/3}$, is smaller than the mean free path, l_0 , of the electrons, the wall collision shortens the relaxation time. For larger particles, the radiation loss which is proportional to the square of the volume V of the particle dissipates much of the energy. We have

$$Q = (\omega\tau)^{-1}(1 + l_0/l) + (2\pi)^{-1}k^3V, \quad (3)$$

where k is the wave vector. The dependence of Q on the size of the cadmium particles is shown in Fig. 2(c).

For photochemical reactions on and near the surface of the metal spheroid, the local transition probability of an instantaneous one-photon reaction is proportional to the square of the local electric-field intensity of the radiation. If we take prolate spheroidal coordinates as

$$\begin{aligned} x &= \frac{c \sin\theta}{\sinh\alpha} \cos\varphi, \\ y &= \frac{c \sin\theta}{\sinh\alpha} \sin\varphi, \quad z = \frac{c \cos\theta}{\tanh\alpha}, \end{aligned} \quad (4)$$

the reaction rate on the surface is proportional to¹⁰

$$E^2 = \frac{E_0^2}{(1 - \omega r^2/\omega^2)^2 + Q^{-2}} \frac{1}{1 - \tanh^2\alpha \cos^2\theta} \times \left[\frac{\cos^2\theta}{\cosh^2\alpha} \left(\frac{\alpha - \sinh\alpha \cosh\alpha}{\alpha - \tanh\alpha} \right)^2 + \sin^2\theta \right]. \quad (5)$$

The relative values of E^2 on the surface of a metal spheroid of $a/b = 1.5$ are shown in Fig. 2(a);

the reaction rate at the pole is ≈ 10 times greater than that at the equator. For metal spheres, the ratio is 4.

Our experimental observations can now be explained by the electric field near the surface of the particle. It has recently been found that Cd metal can be locally photodeposited from adsorbed molecular films.⁹ Thus, an initially spherical particle, covered with a metal-alkyl layer, will grow via photodeposition much faster at its poles than at the equator, because of the anisotropy in E^2 given in Eq. (5). During its growth it will transform from a near spherical to a prolate geometry, giving rise to the elliptical particles shown in Figs. 1(b), 1(c), and 1(d).

The statistics of the final shapes and sizes of the particles could be interpreted as follows. According to the theoretical treatment, the cadmium particles have a resonance with the 257-nm light when $a/b \approx 1$ and Q peaks for $a = 10$ – 30 nm. The particles within this size and shape range will grow quickly into spheroids. When the ratio a/b exceeds 1.5, two competitive effects exist. The reaction rate at the poles is much higher than the spheres, thus making the poles grow even faster. The resonance frequency, however, drops rapidly with increasing ratio a/b . A final, average ratio of 1.8 is reasonable. Moreover, when the size of the particles, defined by a , exceeds 50 nm, the radiation loss will lower drastically the quality factor of resonance; thus an average, final size of $2a \approx 110$ nm is reasonable. The dropoff in Q with small and large particle size is also responsible for the slow growth of both very small and very large particles.

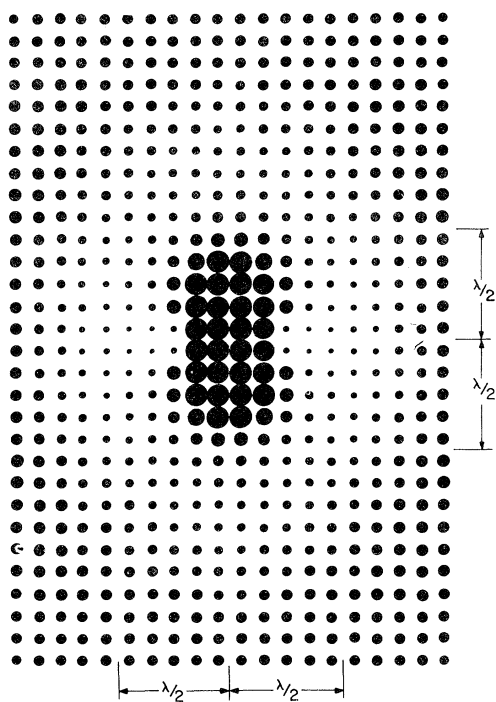


FIG. 3. The distribution of the electric energy density near a resonating metal particle. The area of a spot is proportional to the electric energy density at that point. For clarity, the spot sizes near the center are "clipped" at a value ten times that of the incident field.

The final shape of the photogrown particle can be calculated by a computer simulation by numerically solving the two coupled differential equations for growth along the minor and major axes for various initial sizes. The results of the calculation confirm this conclusion. Finally, the absence of enhanced growth for gold particles is due to the lack of a plasma resonance for gold at 257 nm.

The thin area of deposition which appears around the ellipsoidal particles results from interference of the reradiated electric field with the incident field. A computer simulation of the interference field (Fig. 3) showed a similar geometric pattern. Note the nearly elliptically shaped area of highest intensity and the two small areas of lowest intensity at a distance $\lambda/2$ from the center perpendicular to the incident electric field intensity. These same features are ob-

served in the TEM micrographs of Fig. 1.

In summary, we have shown that direct photochemical reactions can be enhanced by supported metal structures. Our results are important for the understanding of photon-induced surface reactions and for understanding the early stages in metal photodeposition processes.

The authors are grateful to H. Gilgen for his help in photodepositing the Cd films, to R. Kissinger for his help in using the electron microscope, and to A. Szöke and S. Brueck for helpful discussions. In addition, D. W. Lynch generously provided us with information on the optical properties of several metals. This work was supported by the U. S. Army Research Office and the Joint Services Electronics Program under Contract No. DAAG 29-82-K-0080.

¹See, for example, R. P. van Duyne, in *Chemical and Biological Application of Lasers*, edited by C. Moore (Academic, New York, 1979), Vol. 4, Chap. 5; P. M. Platzmann and P. A. Wolff, *Phys. Lett.* **77A**, 381 (1980).

²See, for example, J. Gersten and A. Nitzan, *J. Chem. Phys.* **75**, 1139 (1981), and the literature listed therein.

³A. Nitzan and L. E. Brus, *J. Chem. Phys.* **74**, 537 (1981), and *Chem. Phys.* **75**, 2205 (1981).

⁴J. W. Weaver, C. Krafka, D. W. Lynch, and E. E. Koch, *Optical Properties of Metals*, Physics Data, Vols. 18-1 and 18-2 (Fachinformationszentrum, Karlsruhe, 1981); M. Born and E. Wolf, *Principles of Optics* (MacMillan, London, 1964), pp. 624-627.

⁵T. M. Jalinat, R. N. Hamm, E. T. Arakawa, and R. H. Huebner, *J. Opt. Soc. Am.* **56**, 185 (1966); E. T. Arakawa, R. N. Hamm, W. F. Hanson, and T. M. Jeirek, *Optical Properties and Electronic Structure of Metals and Alloys*, edited by F. Abeles (North-Holland, Amsterdam, 1966), p. 374; J. H. Weaver, D. W. Lynch, and R. Rosei, *Phys. Rev. B* **5**, 2829 (1972).

⁶C. Jonah, P. Chandra, and R. Bersohn, *J. Chem. Phys.* **55**, 1903 (1971).

⁷C. J. Chen and R. M. Osgood, to be published.

⁸K. Kimoto, Y. Kamiya, M. Nonoyama, and R. Uyeda, *Jpn. J. Appl. Phys.* **2**, 702 (1963); K. Kimoto and I. Nishida, *Jpn. J. Appl. Phys.* **6**, 1047 (1967); N. Wada, *Jpn. J. Appl. Phys.* **6**, 553 (1967).

⁹R. M. Osgood and D. J. Ehrlich, *Opt. Lett.* **7**, 385 (1982); S. R. J. Brueck and D. J. Ehrlich, *Phys. Rev. Lett.* **48**, 1678 (1982).

¹⁰C. J. Chen and R. M. Osgood, unpublished.

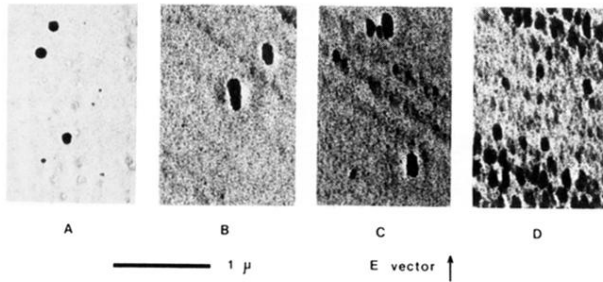


FIG. 1. The TEM photographs of the carbon film with miniature cadmium particles (a) before photochemical deposition, showing randomly distributed spheres; (b), (c), (d) after photochemical deposition, showing elliptical similar growth to similar sizes, well aligned with the electric field of the light.